

Primordial Supernovae and the Assembly of the First Galaxies

Daniel Whalen¹, Bob Van Veelen², Brian W. O’Shea³, and Michael L.
Norman⁴

¹Applied Physics (X-2), Los Alamos National Laboratory, Los Alamos, NM 87545
email: dwhalen@lanl.gov

²Astronomical Institute Utrecht, Princetonplein 5, Utrecht, The Netherlands

³Theoretical Astrophysics (T-6), Los Alamos National Laboratory, Los Alamos, NM 87545

⁴Center for Astrophysics and Space Sciences, University of California at San Diego, La Jolla,
CA 92093

Abstract.

Current numerical studies suggest that the first protogalaxies formed a few stars at a time and were enriched only gradually by the first heavy elements. However, these models do not resolve primordial supernova (SN) explosions or the mixing of their heavy elements with ambient gas, which could result in intervening, prompt generations of low-mass stars. We present multiscale 1D models of Population III supernovae in cosmological minihalos that evolve the blast from its earliest stages as a free expansion. We find that if the star ionizes the halo, the ejecta strongly interacts with the dense shell swept up by the H II region, potentially cooling and fragmenting it into clumps that are gravitationally unstable to collapse. If the star fails to ionize the halo, the explosion propagates metals out to 20 - 40 pc and then collapses, heavily enriching tens of thousands of solar masses of primordial gas, in contrast to previous models that suggest that such explosions ‘fizzle’. Rapid formation of low-mass stars trapped in the gravitational potential well of the halo is unavoidable in these circumstances. Consequently, it is possible that far more stars were swept up into the first galaxies, at earlier times and with distinct chemical signatures, than in present models. Upcoming measurements by the *James Webb Space Telescope (JWST)* and *Atacama Large Millimeter Array (ALMA)* may discriminate between these two paradigms.

Keywords. cosmology: theory—early universe—hydrodynamics—stars: early type—supernovae: individual

1. Introduction

Adaptive mesh refinement (AMR) and smooth particle hydrodynamics methods indicate that primordial stars form in the first cosmological dark matter halos to reach masses of a few $10^5 M_{\odot}$ at $z \sim 20 - 30$, and that due to inefficient H_2 cooling they are likely very massive, 30 - 500 M_{\odot} (Abel et al. 2002, Bromm et al. 2001, Nakamura & Umemura 2001). With surface temperatures of $\sim 10^5$ K and ionizing emissivity rates of 10^{50} s^{-1} , these stars profoundly alter the halos that give birth to them, creating H II regions 2.5 - 5 kpc in radius and sweeping half of the baryons in the halo into a dense shell that grows to the virial radius of the halo by the end of the life of the star, as first pointed out by Whalen et al. (2004) and Kitayama et al. (2004). Recent work shows that a second lower-mass star can form in the relic H II region of its predecessor in the absence of a supernova (Yoshida et al. 2007).

While single stars form consecutively in halos, gravitational mergers consolidate them into larger structures. Numerical attempts to follow this process find that primordial supernovae expel their heavy elements into low-density voids, where star formation is

not possible. The metals return to their halos of origin on timescales of 50 - 100 Myr by accretion infall and mergers and, having been diluted by their expulsion into the IGM, are taken up into later generations of stars relatively slowly. However, the large computational boxes required to follow the formation of halos from cosmological initial conditions prevents them from fully resolving the explosions. Furthermore, the blasts themselves are not properly initialized, being set up as static bubbles of thermal energy rather than the free expansions that actually erupt through the atmosphere of the star.

If the explosion is initialized in an H II region and one is not concerned with the transport of metals or fine structure cooling, thermal ‘bombs’ yield an acceptable approximation to gas motion on kiloparsec scales. However, this approach cannot capture the mixture of heavy elements with ambient gas or the subsequent formation of dense enriched clumps due to metal line cooling for two reasons. First, the thermal bubble does create large pressure gradients that accelerate gas outward into the surrounding medium, but because the ejecta has no initial momentum and dynamically couples to surrounding gas at low density ($\lesssim 1 \text{ cm}^{-3}$), not all the metals are launched out into the halo. Our numerical experiments demonstrate that unphysically large amounts of heavy elements remain at the origin of the coordinate grid when the explosion is implemented in this manner. Second, the early evolution of the thermal pulse is different from that of a free expansion, which exhibits the formation of reverse shocks and contact discontinuities that would destabilize in 3D and cause mixing at fairly small radii. Since dynamical instabilities in the blast that are mediated by line cooling are highly nonlinear, it is crucial to follow them from their earliest stages, something that cannot be accomplished with thermal bubbles.

If instead the progenitor fails to ionize the halo, densities at the center remain high, in excess of 10^8 cm^{-3} . When the supernova is initialized with thermal energy in this environment, all the energy of the blast is radiated away before any of the surrounding gas can be driven outward. Since the energy of the explosion is deposited as heat at the center of the grid, the temperature skyrockets to billions of degrees, instantly ionizing the gas collisionally. Bremsstrahlung and inverse Compton cooling time scales at these densities and temperatures are extremely short, leading earlier studies to erroneously conclude that such blasts ‘fizzle’. In reality, even though 90% of the energy of the explosion may be lost in the first 2 - 3 years, the momentum of the free expansion cannot be radiated away, guaranteeing some propagation of ejecta out into the halo. We present a new series of Population III supernova models in both neutral and ionized cosmological minihalos to address these difficulties.

2. Code Algorithm/Models

We examined the explosion of 15, 40, and 200 M_{\odot} stars (Type II supernovae, hypernovae, and pair-instability supernovae–PISN) in 5.9×10^5 , 2.1×10^6 , and $1.2 \times 10^7 M_{\odot}$ dark matter halos, which span the range in mass in which stars are expected to form by H_2 cooling (Whalen et al. 2008). Each model was carried out in two stages: first, spherically-averaged halo baryon profiles computed from cosmological initial conditions in the Enzo AMR code were imported into the ZEUS-MP code (Whalen & Norman 2006) and photoionized by the star, which is placed at the center of the halo. We then set off the explosion in the H II region of the star, using the Truelove & McKee (1999) free expansion solution for the blast profile. Each free expansion was confined to 0.0012 pc to ensure that the profile enclosed less ambient gas than ejecta mass. The explosion was then evolved with primordial gas chemistry self-consistently coupled to hydrodynamics to follow energy losses from the remnant due to line, bremsstrahlung, and inverse Compton emission in gas swept up by the ejecta. We show H II region and blast profiles in Figure 1.

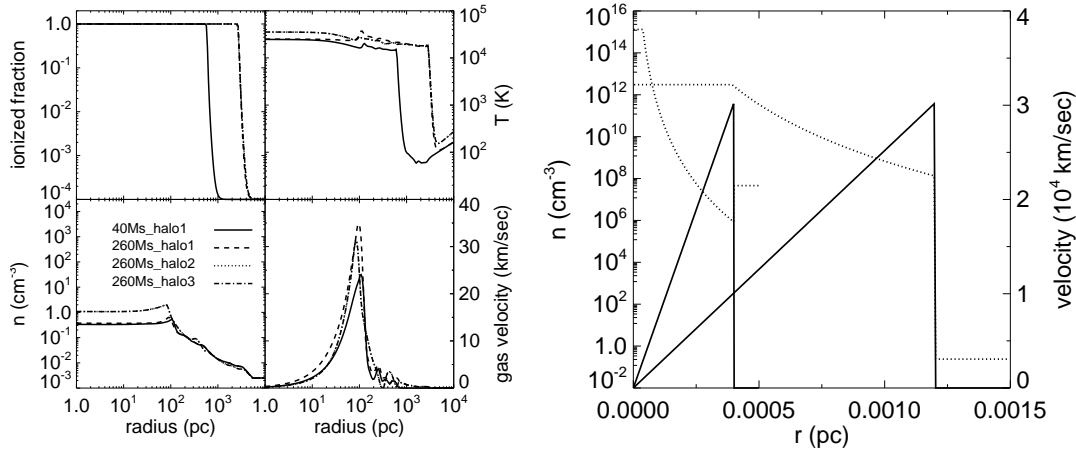


Figure 1. Left panel: H II region profiles of stars that fully ionize their halos. Right panel: Truelove & McKee free-expansion density and velocity (triangular) profiles.

The $200 M_{\odot}$ star fully ionizes the first two halos and partially ionizes the most massive; the 15 and $40 M_{\odot}$ stars fail to ionize the third halo, but either fully or partially ionize the two less massive halos. The explosions evolve along two distinct pathways according to whether they occur in H II regions or in neutral halos.

3. Explosions in H II Regions

Profiles of density, temperature, ionization fraction, and velocity for a $200 M_{\odot}$ PISN in the 5.9×10^5 halo are shown at 31.7, 587, and 2380 yr, respectively, in Figure 2 a-d. At 31.7 yr a homologous free expansion is still visible in the density profile, which retains a flat central core and power-law dropoff. By 2380 yr the remnant has swept up more than its own mass, forming a reverse shock that is separated from the forward shock by a contact discontinuity. In 3D this contact discontinuity will break down into Rayleigh-Taylor instabilities, mixing the surrounding pristine gas with metals at small radii, 15 pc or less. Thus, mixing will occur well before the remnant collides with the shell, which we show in Figure 2 e-h at 19.8 and 420 kyr. The 400 km s^{-1} shock overtakes the 25 km s^{-1} H II region shell at $r = 85 \text{ pc}$ at 61.1 kyr. Its impact is so strong that a second reverse shock forms and separates from the forward shock at 420 kyr. Both shocks are visible in the density and velocity profiles of Figure 2 at 175 and 210 pc. In reality, the interaction of the SN and shell is more gradual: the remnant encounters the tail of the shell at 60 pc at 19.8 kyr, at which time the greatest radiative losses begin, tapering off by 7 Myr with the formation of another reverse shock. More than 80% of the energy of the blast is radiated away upon collision with the shell. Hydrogen Ly- α radiation dominates, followed by inverse Compton scattering, collisional excitation of He^+ and bremsstrahlung, but the remnant also collisionally ionizes H and He in the dense shell. It is clear that the impact of the remnant with the shell will result in a second episode of violent mixing with metals, although dynamical instabilities in the blast will set in well before the collision.

4. Explosions in Neutral Halos

In Figure 3 we show hydrodynamical profiles for a $40 M_{\odot}$ hypernova in the $1.2 \times 10^7 M_{\odot}$ halo. In panels (a) - (d) are shown the formation of the reverse shock between 7.45

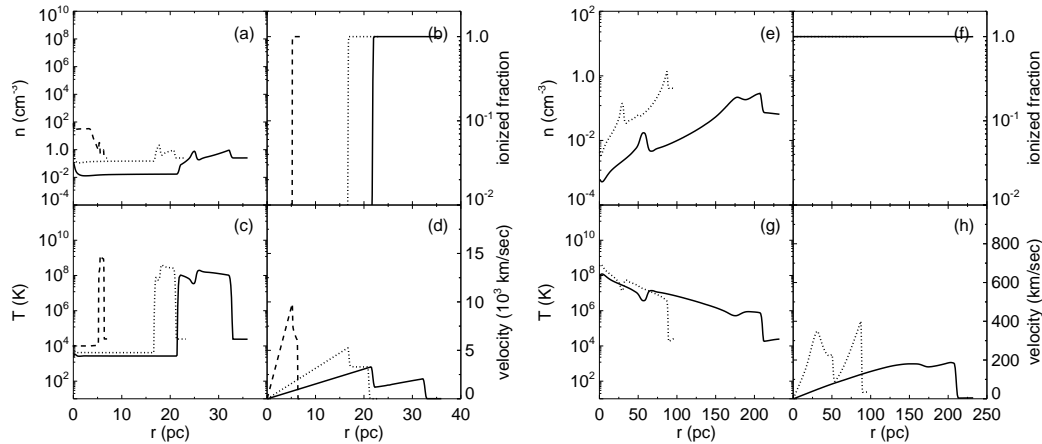


Figure 2. Panels a - d: formation of a reverse shock in a $260 M_{\odot}$ PISN. Dashed: 31.7 yr; dotted: 587 yr; solid: 2380 yr. Panels e - h: collision of the remnant with the H II region shell. Dotted: 19.8 kyr; solid: 420 kyr.

and 17.4 yr. The Chevalier phase is again evident, in which a reverse shock backsteps from the forward shock with an intervening contact discontinuity, but it occurs at much earlier times because much more gas resides at the center of the halo. Heavy element mixing sets in at very small radii in neutral halos. Expansion and fallback of the remnant is evident in panels (e) - (f), in which profiles are taken at 2.14 and 6.82 Myr. The hot bubble reaches a final radius of ~ 40 pc and then recollapses toward the center of the halo. The remnant undergoes several subsequent cycles of expansion and contraction in the gravitational potential of the dark matter, with episodes of large central accretion rates, which we show in the left panel of Figure 4. A few tens of thousands of solar masses will become enriched with metals above the threshold for low-mass star formation, with the likely result being a swarm of low-mass stars gravitationally bound to the dark matter potential of the halo. We show in the right panel of Figure 4 the final outcome of each explosion model.

5. Conclusion

Our 1D survey of primordial supernova remnant energetics in cosmological halos strongly suggest that when metals and metal line cooling are included in the next generation of 3D models, dynamical instabilities will strongly mix the surrounding gas with heavy elements. This may lead to a second, prompt generation of stars forming in either the enriched dense shell of the relic H II region or deeper inside a neutral halo. If so, the first protogalaxies may have had far more stars than in current models. Large infall rates in trapped explosions may also be efficient at fueling the growth of the compact remnant of less massive progenitors, possibly providing the seeds of the supermassive black holes found in most large galaxies today.

References

- Abel, T., Bryan, G. L., & Norman, M. L. 2002, *Science*, 295, 93
 Abel, T., Wise, J. H., & Bryan, G. L. 2007, *ApJL*, 659, L87
 Alvarez, M. A., Bromm, V., & Shapiro, P. R. 2006,
 Bromm, V., Ferrara, A., Coppi, P. S., & Larson, R. B. 2001, *MNRAS*, 328, 969

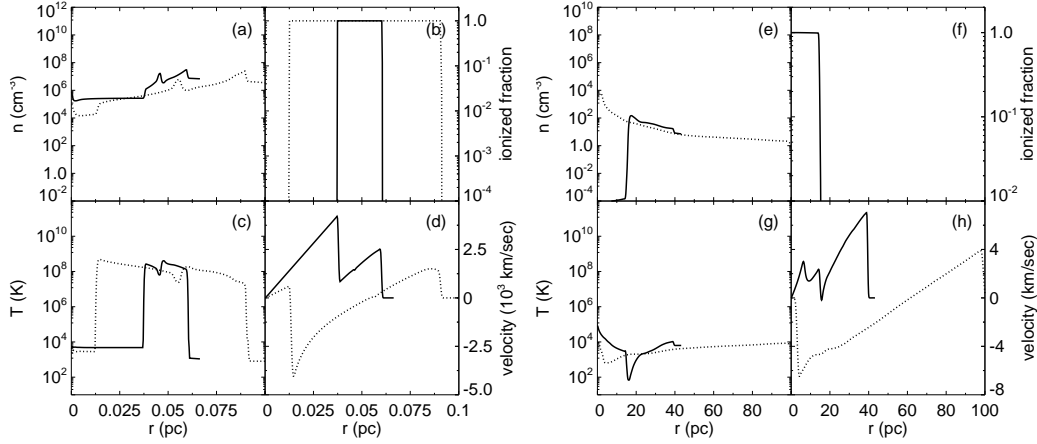


Figure 3. Panels a - d: early flow profiles of a $40 M_{\odot}$ hypernova in a neutral halo. Solid: 7.45 yr; dotted: 17.4 yr. Panels e - h: collapse of the remnant. Dotted: 2.14 Myr; solid: 6.82 Myr.

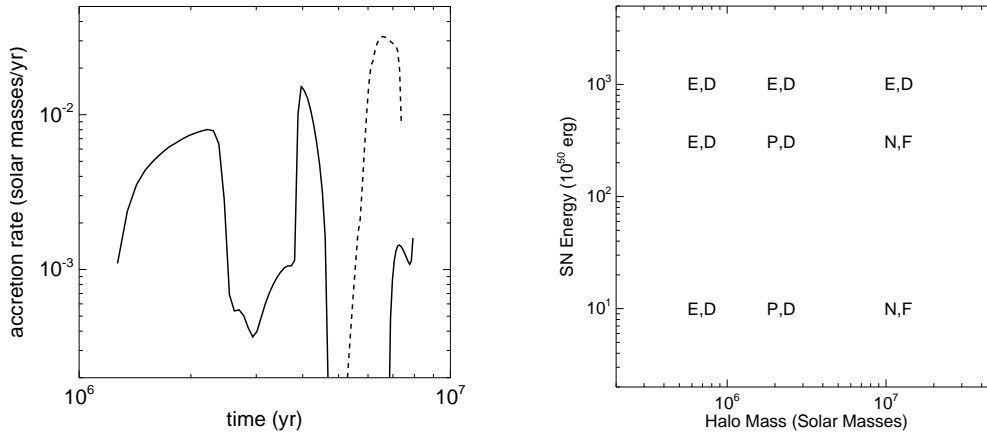


Figure 4. Left panel: Infall rates associated with fallback of the 15 (solid) and 40 (dashed) M_{\odot} remnants in the most massive of the three halos. Right panel: eventual fate of a halo given the indicated explosion energy. The first letter refers to the final state of the halo prior to the explosion; E: photoevaporated; P: partly ionized, defined as the I-front not reaching the virial radius; N: neutral, or a failed H II region. The second letter indicates outcome of the explosion; D: destroyed, or F: fallback.

Kitayama, T., Yoshida, N., Susa, H., & Umemura, M. 2004, *ApJ*, 613, 631

Nakamura, F., & Umemura, M. 2001, *ApJ*, 548, 19

Truelove, J. K., & McKee, C. F. 1999, *ApJS*, 120, 299

Yoshida, N., Oh, S. P., Kitayama, T., & Hernquist, L. 2007, *ApJ*, 663, 687

Whalen, D., Abel, T., & Norman, M. L. 2004, *ApJ*, 610, 14

Whalen, D., & Norman, M. L. 2006, *ApJS*, 162, 281

Whalen, D., van Veelen, B., O'Shea, B. W., & Norman, M. L. 2008, ArXiv e-prints, 801, arXiv:0801.3698